Supplement of Earth Syst. Dynam., 17, 913–928, 2026
https://doi.org/10.5194/esd-17-913-2026-supplement

Earth System Dynamics
Open Access
EGU

Supplement of

Northern high latitudes could become a net carbon source below 2 °C global warming

Rebecca M. Varney et al.

Correspondence to: Rebecca M. Varney (rebecca.varney@natgeo.su.se)

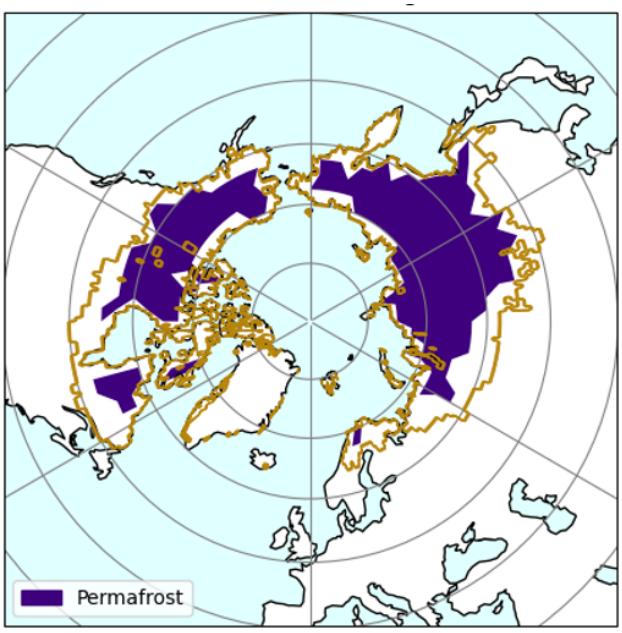

Figure S1. Northern high-latitude region considered in this study, as defined in Hugelius et al. (2024) for RECCAP2. The marked area outlines the entire region and the shaded area represents the location of permafrost in JULES-pf at the start of the simulations in 1850.

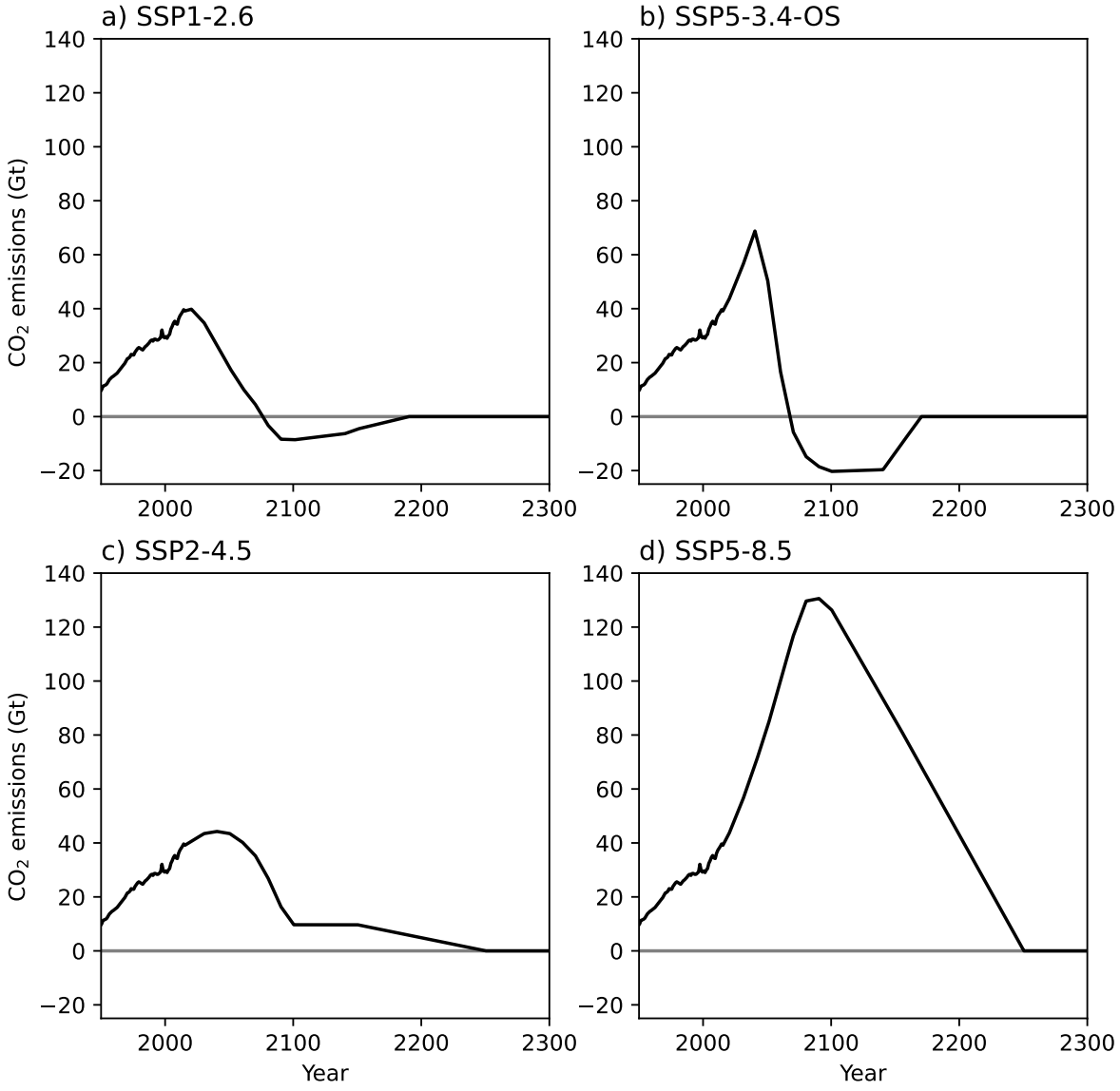

Figure S2. Timeseries of global CO_2 emissions for the SSP scenarios and their extensions to 2300: (a) SSP1-2.6, (b) SSP5-3.4-OS, (c) SSP2-4.5, and (d) SSP5-8.5.

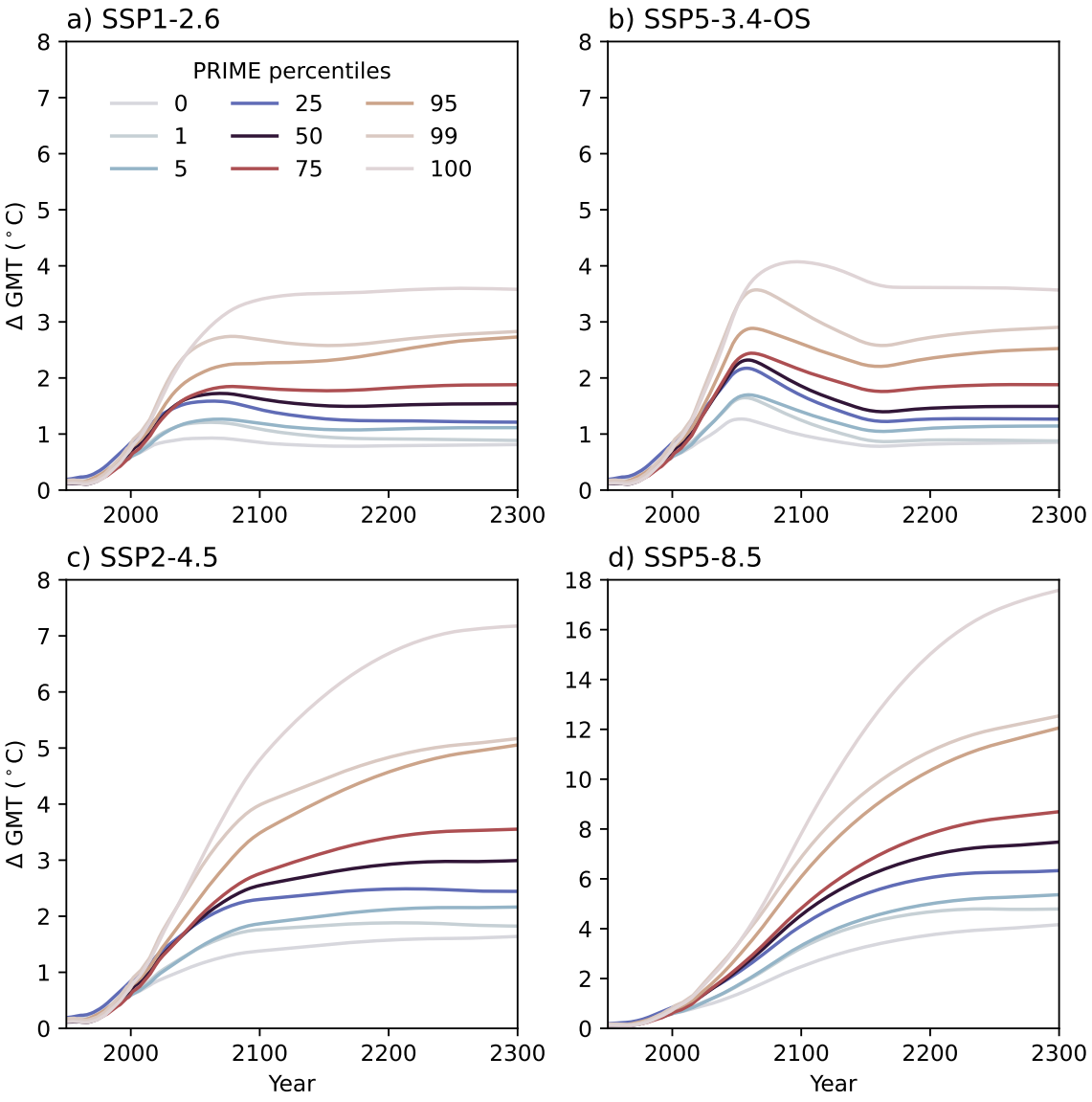

Figure S3. Timeseries of the projected global temperature changes for the SSP scenarios: (a) SSP1-2.6, (b) SSP5-3.4-OS, (c) SSP2-4.5, and (d) SSP5-8.5. Shown for the percentiles produced by PRIME using the mean of the climate patterns (colours).

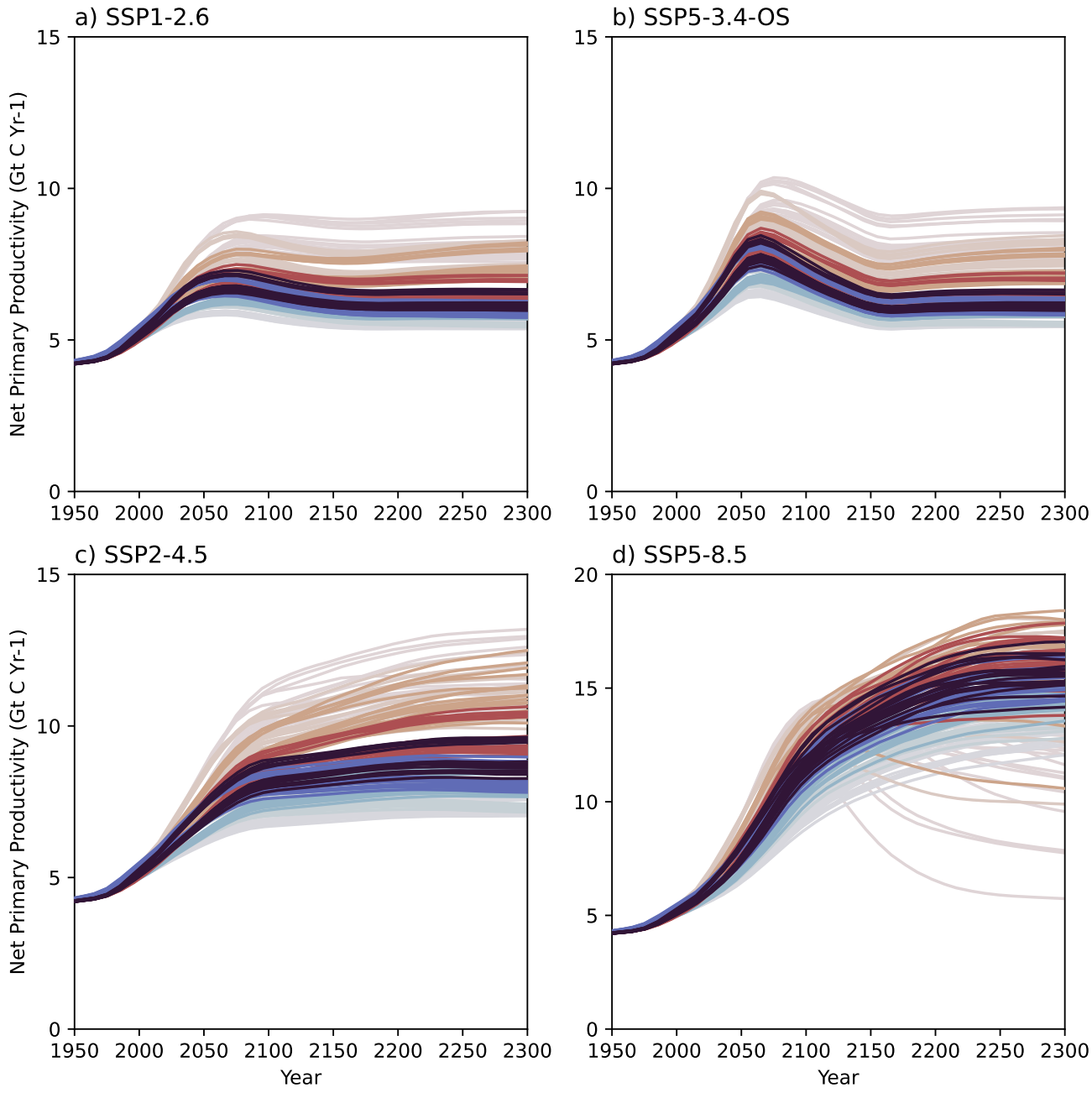

Figure S4. Timeseries of global total Net primary productivity (NPP) for the JULES-pf configuration. The different colours are the different PRIME percentiles and the individual lines within each colour are different spatial patterns of change across the selected CMIP6 ESMs.

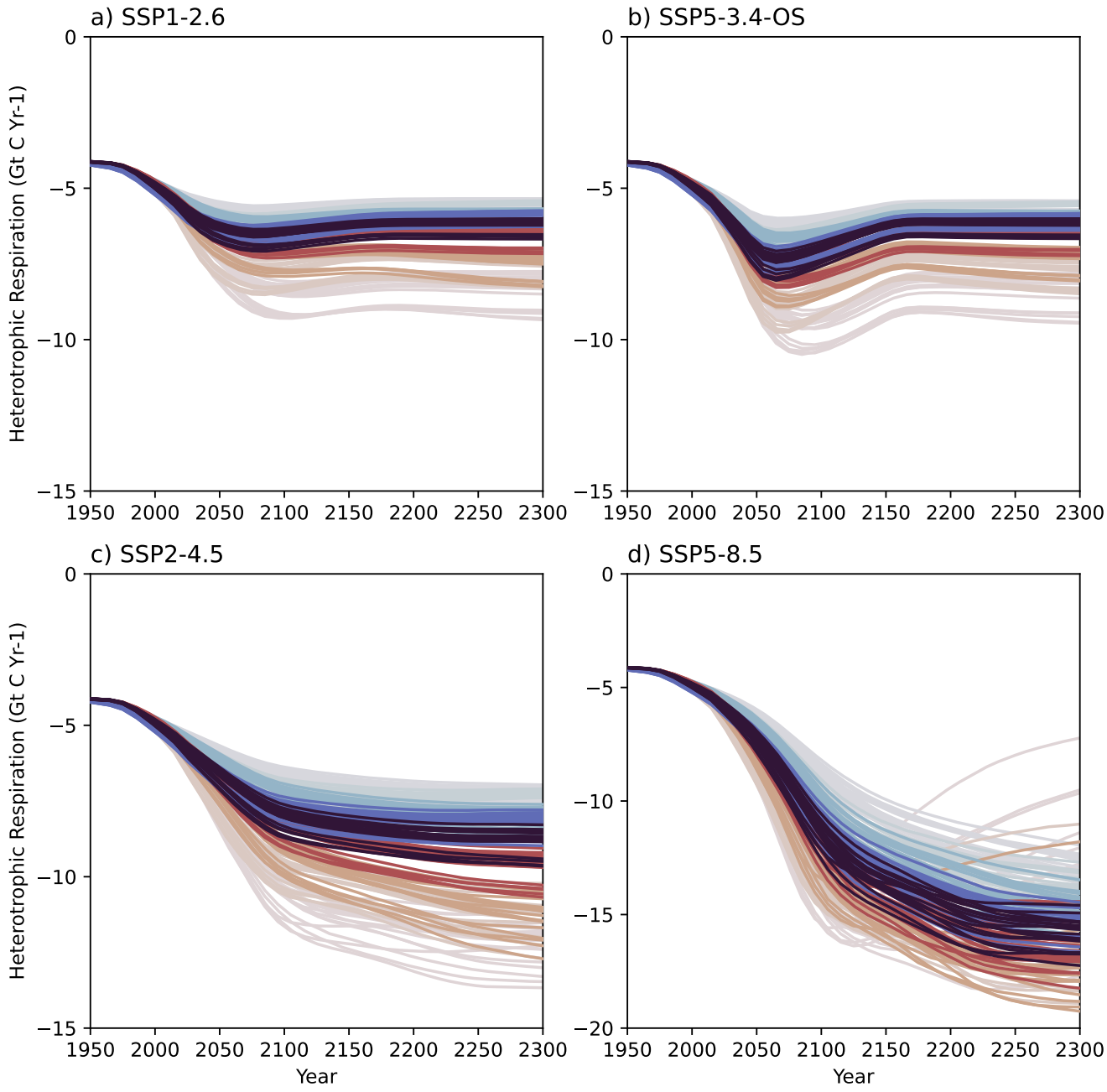

Figure S5. Timeseries of global total heterotrophic respiration (R_h) for the JULES-pf configuration. The different colours are the different PRIME percentiles and the individual lines within each colour are different spatial patterns of change across the selected CMIP6 ESMs.

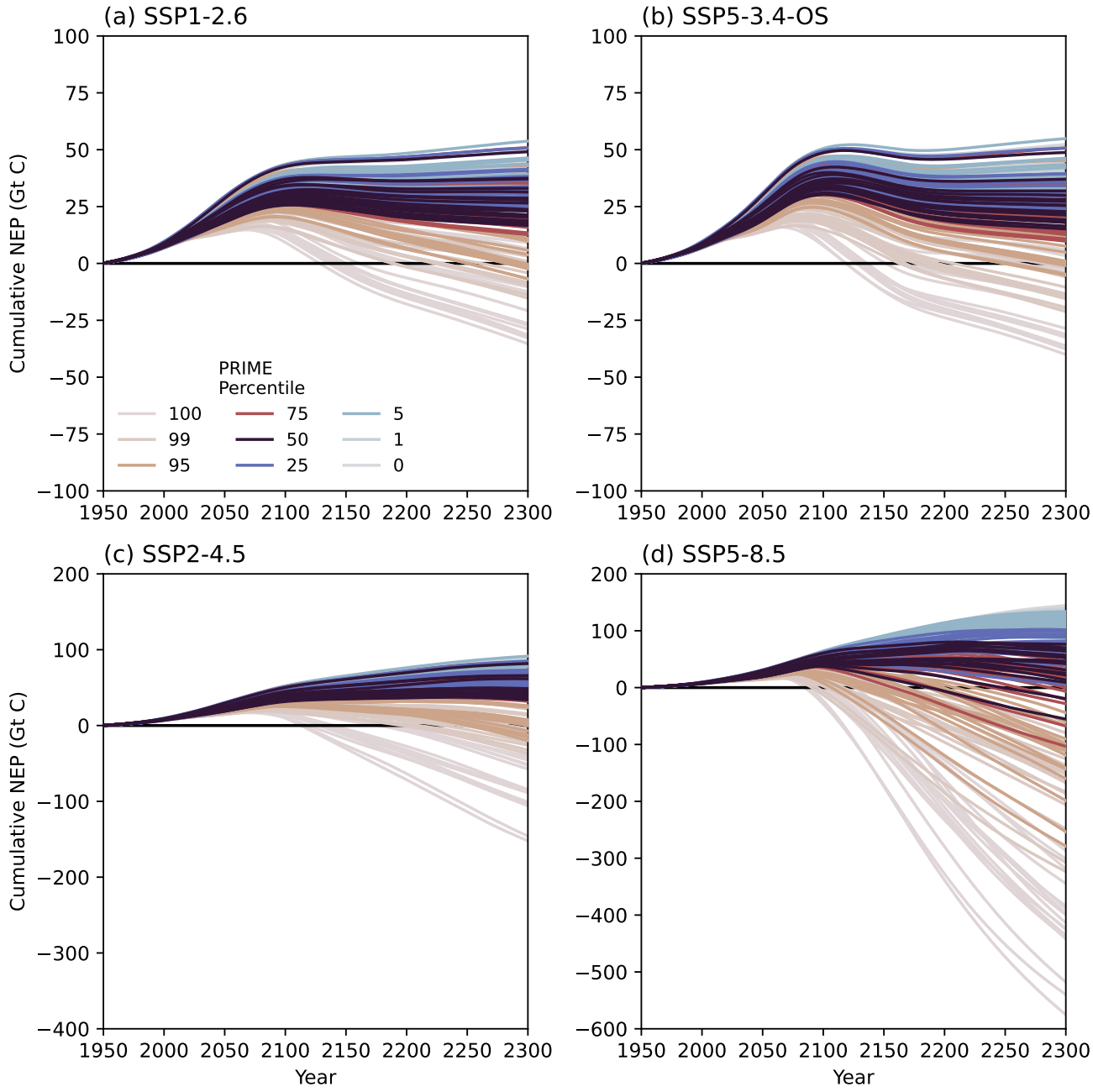

Figure S6. Timeseries of cumulative total Net ecosystem productivity (NEP; Gt C) over the RECCAP2 permafrost region in the JULES-pf configuration, for: (a) SSP1-2.6, (b) SSP5-3.4-OS, (c) SSP2-4.5, and (d) SSP5-8.5. The different colours are for different PRIME percentiles representing a range of climate sensitivities and the individual lines within each colour are different spatial patterns of change across the selected CMIP6 ESMs.

Table S1. The 18 CMIP6 ESMs which were used with the SSP5-8.5 driven climate patterns to drive JULES as part of the PRIME framework.

	Model
1.	ACCESS-CM2
2.	ACCESS-ESM1-5
3.	CNRM-CM6-1
4.	CNRM-CM6-1-HR
5.	CNRM-ESM2-1
6.	CanESM5
7.	EC-Earth3-Veg
8.	FGOALS-g3
9.	HadGEM3-GC31-LL
10.	HadGEM3-GC31-MM
11.	INM-CM4-8
12.	IPSL-CM6A-LR
13.	MIROC-ES2L
14.	MIROC6
15.	MPI-ESM1-2-HR
16.	MPI-ESM1-2-LR
17.	MRI-ESM2-0
18.	UKESM1-0-LL

S1.1 CARDAMOM

CARDAMOM is a model-data fusion framework used to provide an uncertainty bounded systemic-data informed analysis of terrestrial ecosystem carbon cycling. CARDAMOM uses a Bayesian approach within an Adaptive-Proposal Markov Chain Monte Carlo algorithm (Haario et al., 2001; Bloom et al., 2016) to integrate diverse ecological information and their uncertainties to retrieve ensembles of parameters (representing ecosystem traits) for an intermediate complexity process-model of the terrestrial ecosystem carbon and water cycles (DALEC). CARDAMOM-DALEC is applied on a per-pixel basis, meaning that the calibration for each location is a function of the local data, their uncertainties and ecological theory embedded in DALEC and ecological and dynamical constraints (for details see Bloom and Williams, 2015; Bloom et al., 2016; Famiglietti et al., 2021; Smallman et al., 2021). Our pixel-by-pixel approach gives us a unique capability to retrieve spatially explicit parameter (i.e. trait) and uncertainty information, removing the need for plant functional type assumption, instead reflecting real within biome biological variability (Exbrayat et al., 2018). Our analyses can be used to understand the internal carbon cycling dynamics from site scale (Smallman et al., 2017; George-Chacon et al., 2023; Thayamkottu et al., 2024) to large scale evaluations of land surface models not able to directly integrate observations (Caen et al., 2022; Williams et al., 2025).

DALEC is a suite of process-models of varied levels of complexity and process representation, selected to match to the requirements of the analysis of interest and the availability of observations for calibration. The specific version of DALEC used here is DALEC-4 (Smallman et al., 2021), hereafter referred to simply as DALEC. DALEC simulates the states and fluxes of carbon and water in terrestrial ecosystems and their exchanges with the atmosphere. DALEC has four live C pools (labile, foliage, wood (above + below), and fine roots), two dead organic matter pools (litter, soil organic matter (SOM)) and a three soil water pools at varied depths. Carbon uptake, via photosynthesis (gross primary production, GPP), is estimated as a function of meteorology, simulated LAI and available water supply from the roots. GPP is allocated to autotrophic respiration (R_a) and plant tissues based on temporally fixed fractions. The labile pool supports additional seasonal foliage growth as a function of a day-of-year model, while foliage loss is also determined using a day-of-year model (Bloom and Williams, 2015). Wood and fine root turnover follows 1^{st} order kinetics. Decomposition of litter to SOM and heterotrophic respiration (R_h) resulting from the mineralisation of both litter and SOM follow parametrisable 1^{st} order kinetics with an exponential temperature modification. Fire and deforestation / degradation are imposed on DALEC using forcings derived from Earth observations. Fire emissions are determined by imposing a burned fraction and assuming a fraction of the biomass contained in the burned pixel fraction is combusted or converted to litter based on locally calibrated, tissue specific combustion-completeness factors, following Exbrayat et al. (2018). Deforestation / degradation follows a similar approach to fire. Each carbon stock and flux within DALEC is controlled by one or more parameters which are estimated probabilistically by CARDAMOM.

The version of CARDAMOM used here (2003-2024, 0.5 x 0.5 degree, monthly) is described in detail in Smallman et al., (*in prep*) and is submitted to version 14 of the TRENDY model inter-comparison which feeds into the Global Carbon Project 2025 (Friedlingstein et al., 2026). CARDAMOM uses the following observational constraints and uncertainties.

- Monthly MODIS LAI and fAPAR (2003-2023; Myneni et al. (2021)).
- Annual MODIS GPP (2003-2023; Running and Zhao (2021)).
- Annual woody biomass maps (2007, 2010, 2015-2019) merged from Xu et al. (2021).
- Single estimate of the initial soil C content (1 m depth; Hengl et al. (2017)).

- Prior estimate for leaf carbon per unit leaf area (Butler et al., 2017).
- Prior estimate for the carbon use efficiency (NPP/GPP; Collalti and Prentice (2019)).

All variables reported in this manuscript are calculated at the pixel level using the full ensemble information and propagated assuming fully correlated uncertainties. Reported values will be the median, defining the 'most likely' estimate given the assimilated observations and the 95% confidence interval (95% CI) but aggregating in space the pixel level 2.5% and 97.5% quantiles.

References

Bloom, A. and Williams, M.: Constraining ecosystem carbon dynamics in a data-limited world: integrating ecological "common sense" in a model–data fusion framework, Biogeosciences, 12, 1299–1315, https://doi.org/10.5194/bg-12-1299-2015, 2015.

Bloom, A. A., Exbrayat, J.-F., Van Der Velde, I. R., Feng, L., and Williams, M.: The decadal state of the terrestrial carbon cycle: Global retrievals of terrestrial carbon allocation, pools, and residence times, Proceedings of the National Academy of Sciences, 113, 1285–1290, https://doi.org/10.1073/pnas.1515160113, 2016.

Butler, E. E., Datta, A., Flores-Moreno, H., Chen, M., Wythers, K. R., Fazayeli, F., Banerjee, A., Atkin, O. K., Kattge, J., Amiaud, B., Blonder, B., Boenisch, G., Bond-Lamberty, B., Brown, K. A., Byun, C., Campetella, G., Cerabolini, B. E. L., Cornelissen, J. H. C., Craine, J. M., Craven, D., de Vries, F. T., Díaz, S., Domingues, T. F., Forey, E., González-Melo, A., Gross, N., Han, W., Hattingh, W. N., Hickler, T., Jansen, S., Kramer, K., Kraft, N. J. B., Kurokawa, H., Laughlin, D. C., Meir, P., Minden, V., Ülo Niinemets, Onoda, Y., Peñuelas, J., Read, Q., Sack, L., Schamp, B., Soudzilovskaia, N. A., Spasojevic, M. J., Sosinski, E., Thornton, P. E., Valladares, F., van Bodegom, P. M., Williams, M., Wirth, C., and Reich, P. B.: Mapping local and global variability in plant trait distributions, Proceedings of the National Academy of Sciences, 114, E10 937–E10 946, https://doi.org/10.1073/pnas.1708984114, 2017.

Caen, A., Smallman, T. L., de Castro, A. A., Robertson, E., von Randow, C., Cardoso, M., and Williams, M.: Evaluating two land surface models for Brazil using a full carbon cycle benchmark with uncertainties, Climate Resilience and Sustainability, 1, e10, https://doi.org/10.1002/cli2.10, 2022.

Collalti, A. and Prentice, I.: Is NPP proportional to GPP? Waring's hypothesis 20 years on, Tree physiology, 39, 1473–1483, https://doi.org/10.1093/treephys/tpz034, 2019.

Exbrayat, J.-F., Smallman, T. L., Bloom, A. A., Huntley, L. B., and Williams, M.: Inverse Determination of the Influence of Fire on Vegetation Carbon Turnover in the Pantropics, Global Biogeochem. Cy., 32, 1776–1789, https://doi.org/10.1029/2018GB005925, 2018.

Famiglietti, C. A., Smallman, T. L., Levine, P. A., Flack-Prain, S., Quetin, G. R., Meyer, V., Parazoo, N. C., Stettz, S. G., Yang, Y., Bonal, D., Bloom, A. A., Williams, M., and Konings, A. G.: Optimal model complexity for terrestrial carbon cycle prediction, Biogeosciences, 18, 2727–2754, https://doi.org/10.5194/bg-18-2727-2021, 2021.

Friedlingstein, P., O'Sullivan, M., Jones, M. W., Andrew, R. M., Bakker, D. C. E., Hauck, J., Landschützer, P., Le Quéré, C., Li, H., Luijkx, I. T., Peters, G. P., Peters, W., Pongratz, J., Schwingshackl, C., Sitch, S., Canadell, J. G., Ciais, P., Aas, K., Alin, S. R., Anthoni, P., Barbero, L., Bates, N. R., Bellouin, N., Benoit-Cattin, A., Berghoff, C. F., Bernardello, R., Bopp, L., Brasika, I. B. M., Chamberlain, M. A., Chandra, N., Chevallier, F., Chini, L. P., Collier, N. O., Colligan, T. H., Cronin, M., Djeutchouang, L. M., Dou, X., Enright, M. P., Enyo, K., Erb, M., Evans, W., Feely, R. A., Feng, L., Ford, D. J., Foster, A., Fransner, F., Gasser, T., Gehlen, M., Gkritzalis, T., Goncalves De Souza, J., Grassi, G., Gregor, L., Gruber, N., Guenet, B., Gürses, O., Harrington, K., Harris, I., Heinke, J., Hurtt, G. C., Iida, Y., Ilyina, T., Ito, A., Jacobson, A. R., Jain, A. K., Jarníková, T., Jersild, A., Jiang, F., Jones, S. D., Kato, E., Keeling, R. F., Klein Goldewijk, K., Knauer, J., Kong, Y., Korsbakken, J. I., Koven, C., Kunimitsu, T., Lan, X., Liu, J., Liu, Z., Liu, Z., Lo Monaco, C., Ma, L., Marland, G., McGuire, P. C., McKinley, G. A., Melton, J. R., Monacci, N., Monier, E., Morgan, E. J., Munro, D. R., Müller, J. D., Nakaoka, S.-I., Nayagam, L. R., Niwa, Y., Nutzel, T., Olsen, A., Omar, A. M., Pan, N., Pandey, S., Pierrot, D., Qin, Z., Regnier, P., Rehder, G., Resplandy, L., Roobaert, A., Rosan, T. M., Rödenbeck, C., Schwinger, J., Skjelvan, I., Smallman, T. L., Spada, V., Sreeush, M. G., Sun, Q., Sutton, A. J., Sweeney, C., Swingedouw, D., Séférian, R., Takao, S., Tatebe, H., Tian, H., Tian, X., Tilbrook, B., Tsujino, H., Tubiello, F., van Ooijen, E., van der Werf, G. R., van de Velde, S. J., Walker, A. P., Wanninkhof, R., Yang, X., Yuan, W., Yue, X., and Zeng, J.: Global Carbon Budget 2025, Earth System Science Data, 18, 3211–3288, https://doi.org/10.5194/essd-18-3211-2026, 2026.

George-Chacon, S. P., Smallman, T. L., Dupuy, J. M., Hernández-Stefanoni, J. L., Milodowski, D. T., and Williams, M.: Isolating the effects of land use and functional variation on Yucatán's forest biomass under global change, Frontiers in Forests and Global Change, 6, 1204 596, https://doi.org/10.3389/ffgc.2023.1204596, 2023.

Haario, H., Saksman, E., and Tamminen, J.: An adaptive Metropolis algorithm, Bernoulli, 7, 223–242, https://doi.org/7(2): 223-242, 2001.

Hengl, T., Mendes de Jesus, J., Heuvelink, G. B. M., Ruiperez Gonzalez, M., Kilibarda, M., Blagotić, A., Shangguan, W., Wright, M. N., Geng, X., Bauer-Marschallinger, B., Guevara, M. A., Vargas, R., MacMillan, R. A., Batjes, N. H., Leenaars, J. G. B., Ribeiro, E., Wheeler, I., Mantel, S., and Kempen, B.: SoilGrids250m: Global gridded soil information based on machine learning, PLoS one, 12, e0169 748, https://doi.org/10.1371/journal.pone.0169748, 2017.

Hugelius, G., Ramage, J., Burke, E., Chatterjee, A., Smallman, T. L., Aalto, T., Bastos, A., Biasi, C., Canadell, J. G., Chandra, N., Chevallier, F., Ciais, P., Chang, J., Feng, L., Jones, M. W., Kleinen, T., Kuhn, M., Lauerwald, R., Liu, J., López-Blanco, E., Luijkx, I. T., Marushchak, M. E., Natali, S. M., Niwa, Y., Olefeldt, D., Palmer, P. I., Patra, P. K., Peters, W., Potter, S., Poulter, B., Rogers, B. M., Riley, W. J., Saunois, M., Schuur, E. A. G., Thompson, R. L., Treat, C., Tsuruta, A., Turetsky, M. R., Virkkala, A.-M., Voigt, C., Watts, J., Zhu, Q., and Zheng, B.: Permafrost region greenhouse gas budgets suggest a weak CO2 sink and CH4 and N2O sources, but magnitudes differ between top-down and bottom-up methods, Global Biogeochemical Cycles, 38, e2023GB007 969, https://doi.org/10.1029/2023GB007969, 2024.

Myneni, R., Knyazikhin, Y., and Park, T.: MODIS/Terra Leaf Area Index/FPAR 8-Day L4 Global 500m SIN Grid V061 [Data set], NASA Land Processes Distributed Active Archive Center. https://doi.org/10.5067/MODIS/MOD15A2H.061, 2021.

Running, S. and Zhao, M.: MODIS/Terra Net Primary Production Gap-Filled Yearly L4 Global 500m SIN Grid V061 [Data set], NASA Land Processes Distributed Active Archive Center. https://doi.org/10.5067/MODIS/MOD17A3HGF.061, 2021.

Smallman, T., Exbrayat, J.-F., Mencuccini, M., Bloom, A., and Williams, M.: Assimilation of repeated woody biomass observations constrains decadal ecosystem carbon cycle uncertainty in aggrading forests, Journal of Geophysical Research: Biogeosciences, 122, 528–545, https://doi.org/10.1002/2016JG003520, 2017.

Smallman, T. L., Milodowski, D. T., Neto, E. S., Koren, G., Ometto, J., and Williams, M.: Parameter uncertainty dominates C-cycle forecast errors over most of Brazil for the 21st century, Earth System Dynamics, 12, 1191–1237, https://doi.org/10.5194/esd-12-1191-2021, 2021.

Thayamkottu, S., Smallman, T. L., Pärn, J., Mander, Ü., Euskirchen, E. S., and Kane, E. S.: Greening of a boreal rich fen driven by CO2 fertilisation, Agricultural and Forest Meteorology, 359, 110 261, https://doi.org/10.1016/j.agrformet.2024.110261, 2024.

Williams, M., Milodowski, D. T., Smallman, T. L., Dexter, K. G., Hegerl, G. C., McNicol, I. M., O'Sullivan, M., Roesch, C. M., Ryan, C. M., Sitch, S., and Valade, A.: Precipitation–fire functional interactions control biomass stocks and carbon exchanges across the world's largest savanna, Biogeosciences, 22, 1597–1614, https://doi.org/10.5194/bg-22-1597-2025, 2025.

Xu, L., Saatchi, S. S., Yang, Y., Yu, Y., Pongratz, J., Bloom, A. A., Bowman, K., Worden, J., Liu, J., Yin, Y., Domke, G., McRoberts, R. E., Woodall, C., Nabuurs, G.-J., de Miguel, S., Keller, M., Harris, N., Maxwell, S., and Schimel, D.: Changes in global terrestrial live biomass over the 21st century, Science Advances, 7, eabe9829, https://doi.org/10.1126/sciadv.abe9829, 2021.